

UNCLASSIFIED

Defense Technical Information Center  
Compilation Part Notice

ADP013691

TITLE: Large Eddy Simulation of a Rib-Roughened Turbulent Channel Flow with Heat Transfer and Property Variations

DISTRIBUTION: Approved for public release, distribution unlimited

This paper is part of the following report:

TITLE: DNS/LES Progress and Challenges. Proceedings of the Third AFOSR International Conference on DNS/LES

To order the complete compilation report, use: ADA412801

The component part is provided here to allow users access to individually authored sections of proceedings, annals, symposia, etc. However, the component should be considered within the context of the overall compilation report and not as a stand-alone technical report.

The following component part numbers comprise the compilation report:

ADP013620 thru ADP013707

UNCLASSIFIED

# LARGE EDDY SIMULATION OF A RIB-ROUGHENED TURBULENT CHANNEL FLOW WITH HEAT TRANSFER AND PROPERTY VARIATIONS

NING MENG AND RICHARD H. PLETCHER

*Department of Mechanical Engineering  
Iowa State University, Ames, Iowa 50011*

**Abstract.** Turbulent channel flow with a rib-roughened wall has been computed with constant heating rate using large eddy simulation. An implicit, second order accurate finite volume scheme was used to solve the time dependent filtered set of equations to determine large eddies, while a dynamic subgrid-scale model was used to account for the subgrid scale effects. A dynamic Prandtl number was introduced to calculate subgrid scale heat transfer. The effects of strong heating on the rib-roughened wall were investigated and Nusselt numbers were computed and compared with experimental data. The instantaneous plots revealed the influence of turbulent heat transfer on velocity, temperature and vorticity in this particular geometry.

## 1. Introduction

Engineers are using three different approaches to cope with turbulence. In industry, Reynold average Navier-Stokes (RANS) methods employing two equation models are widely used in a variety of forms. Direct numerical simulation is mainly used in academic research. Large Eddy Simulation (LES) which originated in academia tends to be a more and more useful analysis tool for industry in recent years. Several commercial codes (such as FLUENT and StarCD) have implemented some types of LES models. LES resolves all the energy-carrying large eddies, but models small eddies with length scales smaller than the grid size. This equips LES with the ability to analyze complex three dimensional time dependent flows at a moderate computational cost where RANS simulations usually fail.

The rib-roughened channel flow is a good test case for LES simulation due to its complex flow features, such as flow separations, recirculation zones, and re-attachment. Cooling in gas turbine blades is a potential application for this kind of flow. Early work was done by Ciofalo and Collins [1] for a rib-roughened channel using the Smagorisky model and a commercial CFD code employing an incompressible flow formulation. Yang and Ferziger [2] used a dynamic subgrid-scale model to simulate a turbulent flow over an obstacle the geometry of which is different from Ciofalo's case. Dailey [3] developed a compressible formulation for large eddy simulation and applied it to the simulation of a compressible channel flow with heat transfer. Further, Meng and Pletcher [4] calculated an isothermal flow case similar to that of Ciofalo and Collins but using dynamic SGS model and a finer grid. This paper is a continuation of that research and considers effects of heat transfer and property variations.

## 2. Problem Description

The problem of interest is the turbulent flow and heat transfer in a two-dimensional plane channel with a periodic array of transverse square ribs on one wall. The simulation was set up such that comparisons could be made to the experimental data of Drain et al. [5] and Bates et al. [6], who made detailed mean and fluctuating velocity measurements. The blockage ratio, which is the ratio of the rib height,  $h$ , to channel height,  $H$ , was  $h/H = 0.2$ . The pitch-to-height ratio of the ribs was 7.2, where the pitch,  $P$ , is the streamwise spacing of the ribs. This value of pitch-to-height ratio was consistently found empirically to yield the greatest enhancement of heat transfer rates [1]. The nominal Reynolds number based on hydraulic diameter ( $D_h = 4\delta$ ) and bulk velocity was  $Re_D = 20,000$ .

For simulations with heat transfer, a constant heat flux,  $q_w = \frac{q_w^*}{C_p \rho_{ref} \bar{U}_{ref} T_{ref}}$ , was applied to both the lower wall and the upper wall. On the front, top, and back surfaces of the rib, a constant heat flux,  $q_{w,rib}$ , was applied with a magnitude that was one-third of the heat flux on the lower wall,  $q_w$ . Consequently, the total heat added to the ribbed channel was the same as for a smooth channel with no ribs and wall heat flux,  $q_w$ . For the simulations presented here,  $q_w = 0.002$ , and  $q_{w,rib} = 0.000667$ .

The computational domain only contained one rib. This section was assumed to be embedded in a periodic array of many ribs in a fully developed flow, which permitted the use of periodic or step periodic boundary conditions in the streamwise direction.

## 2.1. NUMERICAL PROCEDURE

A system of Favre-filtered Navier-Stokes equations was solved using a dynamic sub-grid scale model. The details can be found in Dailey's Ph.D. thesis [3]. The simulations were primarily run with the dual time-stepping LU-SGS scheme with the solution domain divided into 8 blocks for the coarse grid, and 16 blocks for the fine grid. The fine grid simulations were run with 17 processors (one for master node, sixteen for slave nodes) on the IBM-SP2 and required about 10 - 12 hours of wall clock time per 10,000 time steps, depending on the number of subiterations required for each step in physical time.

For the solid walls, including the upper and lower walls and rib surfaces, the no-slip velocity and zero normal pressure gradient boundary conditions were enforced. The wall temperature was determined from the specified heat flux. All solution variables were assumed to be periodic in the  $z$  direction, the only homogeneous direction for this flow. In the streamwise direction, the  $x$ -momentum,  $v$  and  $w$  velocities, and periodic component of the pressure,  $p_p$ , were assumed to be periodic. The mean pressure gradient parameter was adjusted at each time step to maintain the desired mass flow rate. The temperature was assumed to be stepwise periodic, with  $\Delta T_x$  given by

$$\Delta T_x = \frac{q_w L_x}{2(\dot{m}/L_y L_z)} \quad (1)$$

where  $L_y = 2$  and  $L_z = \pi$ .

After the turbulent flow was deemed to be statistically stationary, the simulation was run another 10,000 time steps to compute the ensemble averaged turbulence statistics.

## 2.2. GRID AND RUN PARAMETERS

The dimensions of the computational domain were  $7.2h \times 5h \times 7.85h$ , or  $2.88\delta \times 2\delta \times \pi\delta$ , in the  $x, y, z$  directions, respectively. The coarse grid used  $40 \times 32 \times 24$  control volumes, with 8 cells on each surface of the rib. The fine grid consisted of  $80 \times 64 \times 48$  control volumes, with 16 cells on each surface of the rib. The fine grid is shown in Fig.1. The nondimensional time step was 0.01.

## 3. Results

### 3.1. MEAN AND FLUCTUATING VELOCITY PROFILES

The mean streamwise velocity profiles, normalized by the average bulk velocity on the top of the rib, are depicted in Figs. 2 and 3 at planes A and

B, respectively. Plane A was located mid-way between the ribs, and plane B was located on the middle of the rib top surface. Both experimental data and current simulation results are shown to facilitate the comparison. From these two figures, it can be seen that both coarse-grid results and fine-grid results agree reasonably well with the experimental data in predicting averaged velocity, although fine-grid results are slightly better.

The root-mean-square (*rms*) of the streamwise velocity fluctuations are shown in Figs. 4 and 5. In the prediction of velocity fluctuations in section A, the fine-grid result shows much better agreement with experimental data, even though both results underestimate the velocity fluctuations to some extent. For section B, the fine-grid result captures precisely the peak value near the top of the rib, and continues to be closer to the experimental data than the coarse-grid result. It seems that the fine grid is necessary to calculate the turbulent statistics, e.g. velocity fluctuations, accurately.

### 3.2. HEAT TRANSFER PARAMETERS

The local Nusselt number distribution is shown in Fig. 6, compared to the experimental data of Lockett and Collins [7] at two different Reynolds numbers. The distance along the lower wall of the channel, including the rib surfaces, is represented by  $x$ , and the location of the lower-front corner of the rib is  $x_{le}$ . The normalized Nusselt number distribution, as shown in Fig. 7, used the average Nusselt number as the normalization factor, which is defined as below

$$Nu_{D,avg} = \frac{1}{S} \int_0^S Nu_D(s) ds \quad (2)$$

where  $S$  is the distance along the lower wall, including the rib surfaces. The LES prediction of Nusselt number agrees quite well with experimental data. It reproduced the overall streamwise profile of  $Nu_D$ , with a local maximum immediately upstream of the rib, a global maximum immediately adjacent to the left-upper corner of the rib, and a local minimum immediately downstream of the rib. The fine grid results performed slightly better than coarse grid ones, in particular, in the prediction of the peak values. In Fig. 7, use of the normalized Nusselt number permits comparison of results obtained from different Reynolds numbers. The examination of the profiles reveals that the LES simulation is in very good agreement with experimental data, except that the maximum value of  $Nu_D$  is slightly underestimated. Note that there is an increase of Nusselt number near the trailing edge of the rib for the experimental results ( $Re_D = 29,870$ ), probably due to a recirculation zone that develops on top of the rib at high Reynolds numbers.

### 3.3. ENSEMBLE AVERAGED AND INSTANTANEOUS CONTOURS

Some ensemble averaged and instantaneous contours for a rib-roughened channel flow with heat transfer are presented in this section.

Figure 8 shows mean velocity vectors with a ensemble averaged contour of  $u$  velocity as the background. This plot was created based on the simulation results without heat transfer for the purpose of comparison. A large recirculation zone behind the rib and a smaller recirculation zone in front of the rib are evident. A large fraction of the region between the ribs is in the recirculation zone for the current pitch-to-height ratio. Drain and Martin [5] reported a reattachment length of  $4.3h$ . The present simulation gives a reattachment length of  $4.2 - 4.3h$ .

A 3D geometric representation of this flow (instantaneous  $u$  velocity) is shown in Fig. 9. A cutting plane is located midway in the spanwise direction. The instantaneous velocity contours are very irregular because of the nature of turbulence.

The following figures show the contours of a variety of variables on two cutting planes, which are located at 8% and 92% channel height, respectively, and parallel to the top or bottom walls. Figure 10 reports the instantaneous  $u$  velocity. On the top cutting plane, there are streak patterns, which are characteristics for the small-scale turbulent structure near the wall. On the bottom cutting plane, no obvious streak pattern can be found even though there are still some variations of  $u$  velocity. The existence of recirculation area before and after the rib is thought to be the reason for this streak deterioration.

The instantaneous temperature is presented in Fig. 11. The top cutting plane is uniformly and moderately heated. The bottom cutting plane, however, has a large cool region upstream of the rib and a small hot region downstream of the rib followed by another cool region.

The magnitude of vorticity is reported in Fig. 12. There exist some streak structures of vorticity on the top cutting plane, but the vorticity is weak and smooth on the bottom cutting plane except a narrow area immediately before the front surface of the rib. The recirculation of flow is not conducive to the formation of streak structure of vorticity.

## 4. Conclusions

The simulation of turbulent flow and heat transfer of air in a planar channel with transverse square ribs on one wall was attempted. Very good agreement between fine grid results and experimental data were obtained in predicting velocity and velocity fluctuations. Coarse grid results agree well with experimental data in velocity profiles but not as well as the fine grid results in velocity fluctuation profiles. The Nusselt number profiles obtained

from the current simulation agree reasonably well with experimental data which tends to validate the current SGS model for turbulent heat transfer. The instantaneous contours of some important variables, e.g.  $u$  velocity, temperature, and vorticity, were presented and analyzed. It is found that the recirculation of flow has a negative impact on the formation of streak structure near the wall.

## 5. Acknowledgments

This research was supported in part by the Air Force Office of Scientific Research under grants F49620-94-1-0168 and F49620-00-1-0229 and by the National Science Foundation under grants CTS-9414052 and CTS-9806989. The use of computer resources provided by the Minnesota Supercomputing Institute are gratefully acknowledged.

## References

1. Ciofalo, M. and Collins, M., 1992, "Large eddy simulation of turbulent flow and heat transfer in plane and rib-roughened channels", *International Journal for Numerical Methods in Fluids*, Vol. 15, pp. 453-489.
2. Yang, K. and Ferziger, J., 1993, "Large eddy simulation of turbulent obstacle flow using a dynamic subgrid-scale model", *AIAA Journal*, Vol. 31, pp. 1406-1413.
3. Dailey, L., 1997, "Large eddy simulation of turbulent flows with variable property heat transfer using a compressible finite volume formulation", Ph.D Thesis, Iowa State University.
4. Meng, N., Pletcher, R., and Simons, T., 1999, "Large eddy simulation of a turbulent channel flow with a rib-roughened wall", AIAA 99-0423, 37th AIAA Aerospace Sciences Meeting and Exhibit, January 11-14, 1999/Reno, NV.
5. Drain, L. and Martin, S., 1985, "Two component velocity measurement of turbulent flow in a ribbed-wall flow channel", *Proceedings of the International Conference on Laser Velocimetry - Advances and Applications*, Manchester, U.K.
6. Bates, C., Yeoman, M., and Wilkes, N., 1983, "Non-intrusive measurements and numerical comparison of the axial velocity components in two-dimensional flow channel for backward-facing step and a rib-roughened surface", Harwell Report AERE-R 10787.
7. Lockett, J. and Collins, M., 1990, "Holographic interferometry applied to rib-roughness heat transfer in turbulent flow", *International Journal of Heat and Mass Transfer*, Vol. 33, pp. 2439-2449.

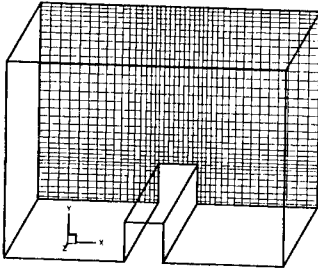


Figure 1. Computational grid for rib-roughened channel flow

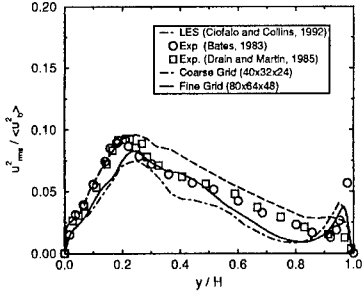


Figure 4. rms streamwise velocity fluctuations normalized by bulk velocity for Section A

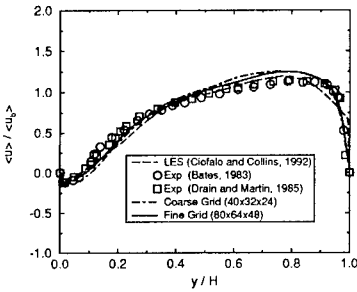


Figure 2. Mean streamwise velocity normalized by bulk velocity for Section A

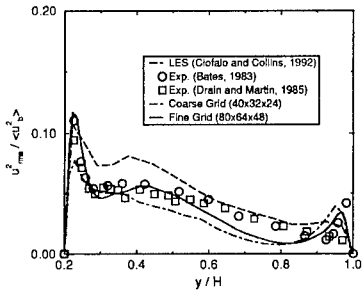


Figure 5. rms streamwise velocity fluctuations normalized by bulk velocity for Section B

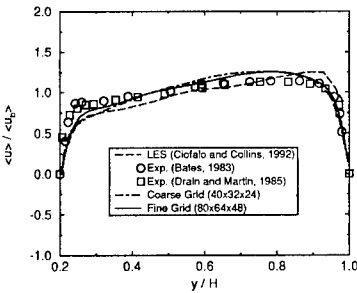


Figure 3. Mean streamwise velocity normalized by bulk velocity for Section B

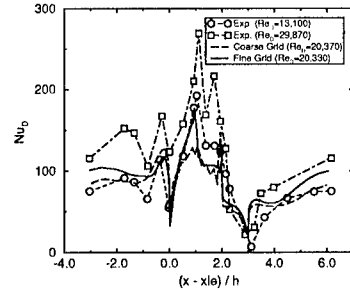


Figure 6. Local Nusselt number compared to experimental data of Lockett and Collins (1990)

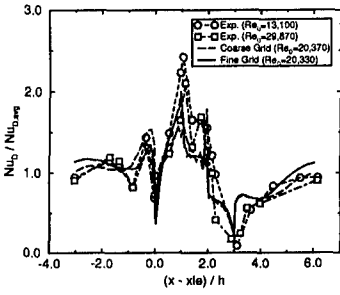


Figure 7. Normalized Nusselt number compared to experimental data of Lockett and Collins (1990)

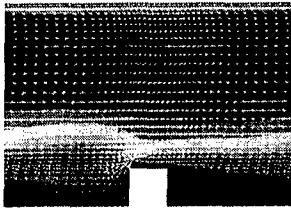


Figure 8. Mean velocity vectors

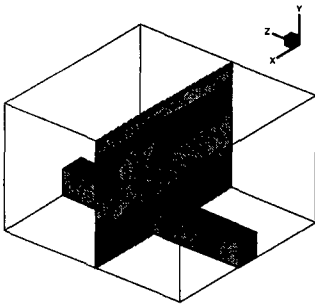


Figure 9. 3D configuration

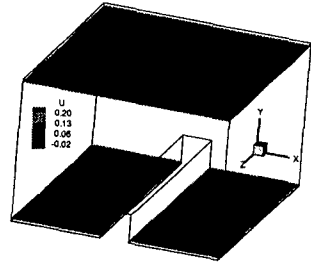


Figure 10. Instantaneous  $u$  velocity

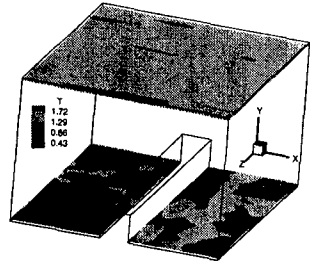


Figure 11. Instantaneous temperature

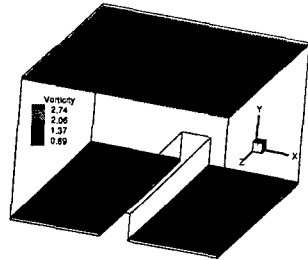


Figure 12. Instantaneous vorticity